DALTON

Effect of guest molecules, metal ions and linker length on the assembly of chiral [2 + 2] metallomacrocycles: solution studies and crystal structures

Mark A. Houghton, Alexander Bilyk, Margaret M. Harding,* Peter Turner and Trevor W. Hambley

School of Chemistry, University of Sydney, N.S.W. 2006, Australia

Eight new 2,2′-bipyridines, containing functionalised acetylenes at the 6 position, have been prepared. The azido derivatives were used to prepare three compounds L^1, L^2 and L^3, which contain pyromellitimide spacers connected to 6,6′-disubstituted 2,2′-bipyridines with propynyl, butynyl and propynyloxy linkers respectively, *via* iminophosphoranes. In the presence of an equimolar amount of zinc(II) triflate (trifluoromethanesulfonate), L^1 was assembled exclusively into the chiral [2 + 2] metallomacrocycle $[Zn_2L^1_2]^{4+}$ at low concentrations (<10 mmol dm^{-3}) or in the presence of an aromatic guest molecule S, which stabilises the complex through binding in the cavity of the metallomacrocycle. The crystal structures of diquabis{*N*,*N*′-bis[3-(6′-methyl-2,2′-bipyridine-6-yl)-prop-2-ynyl]naphthalene-1,8:4,5-tetracarboximide}dizinc tetrakis(triflate) $[Zn_2L^1_2][CF_3SO_3]_4\cdot 2H_2O$, containing either *p*- or *o*-dimethoxybenzene bound in the cavity, were determined by X-ray diffraction methods. In both cases the crystals were extremely fragile and there was extensive disorder of substrate and solvate molecules and the triflate counter ions in channels in the lattice. These structures, while of limited quality, confirm the identity of the complexes, and reveal several substrate-dependent differences. Comparison of the two structures provided clear evidence for the metallomacrocycle adjusting its shape and dimensions to accommodate optimum binding of the substrate through π-stacking/electrostatic interactions, and provides the first example of a metallosupramolecular complex in which the cavity size is determined by the bound substrate. The assembly of the chiral [2 + 2] metallomacrocycle was also achieved with L^1 and cadmium(II) and L^1 and copper(I) in the presence of >20 equivalents of *m*-dimethoxybenzene. In contrast, L^2 and L^3 formed zinc(II) complexes which gave only broadened NMR spectra consistent with equilibrating mixtures of oligomers. The different results obtained with L^1, L^2 and L^3 highlight the importance of the rigid propargyl(prop-2-ynyl) linker in directing the outcome of the assembly process.

The assembly of molecular squares, in which transition-metal ions form the corners of the square,[1,2] as well as metallomacrocycles assembled from organic ligands and transition-metal ions,[3] has received a great deal of attention in recent years. The major aim of these studies has been to identify key building blocks that allow the efficient and controlled assembly of metallosupramolecular structures. Substrates with the potential for inclusion in the cavities of these structures have been selected on examination of the dimensions of the cavities once they have been formed.

In contrast to these previous reports, we have designed bis(bipyridyl) ligands that can be assembled into metallomacrocycles containing multiple recognition sites that may be fine-tuned.[4,5] To this end, ligand L^1 was shown to assemble exclusively into the helical [2 + 2] metallomacrocycle in the presence of Zn^{II}, with an aromatic substrate bound in the cavity, shown in Scheme 1.[5] While the stereochemistry of the metallomacrocycle was assigned using variable-temperature NMR spectroscopy, the nature of the substrate-dependent assembly of the chiral metallomacrocycle was not fully understood. We now report X-ray crystallographic structures of two zinc(II) complexes that confirm our previous NMR assignment,[5] and provide evidence of the capacity of the metallomacrocycle to adjust its binding cavity according to the shape and electronic characteristics of the bound substrate. We also report the effect of metal ions, the length of the linker separating the bipyridyl groups and the aromatic spacer (ligands L^2 and L^3), and the substrate S on the outcome of the assembly process.

Results and Discussion

Ligand synthesis

All ligands were prepared *via* the common intermediate **I** which

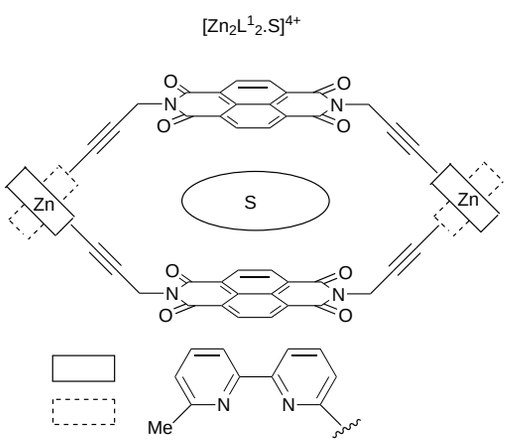

Scheme 1 Representation of the helical [2 + 2] metallomacrocycle formed from two strands of ligand L^1 and two zinc(II) ions in the presence of a guest molecule S

was prepared by Pd^{II}-catalysed coupling of 6-methyl-2-trimethylstannylpyridine[6] and 2,6-dibromopyridine. The synthesis of **I** has been reported previously by coupling of a pyridyl sulfoxide and 2-bromo-6-lithiopyridine,[7] although full characterisation of the product has not been reported. In our hands the route followed in this work was more efficient and reproducible. While some 6,6″-dimethyl-2,2′:6′,2″-terpyridine was also formed as a by-product in the reaction, this was removed by chromatography.

The bromobipyridine **I** was converted into the aminobipyridine **VI** under standard palladium coupling conditions with the propargyl (prop-2-ynyl) amine **II** (Scheme 2). However, this reaction was not reproducible, and highly variable yields were obtained (10–50%) most likely due to the presence of the

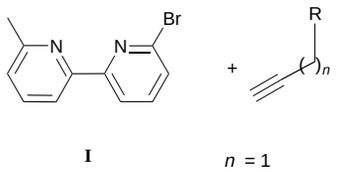

I

n = 1
II R = NH_2
III R = OH

n = 2
IV R = NH_2
V R = OH

n = 1
VI R = NH_2
VII R = OH
VIII R = O_3SMe
IX R = N_3
X R = Br

n = 2
XI R = OH
XII R = O_3SMe
XIII R = N_3

Scheme 2 (*i*) Pd^0, $NHPr^i_2$, Cu^I, tetrahydrofuran (thf)

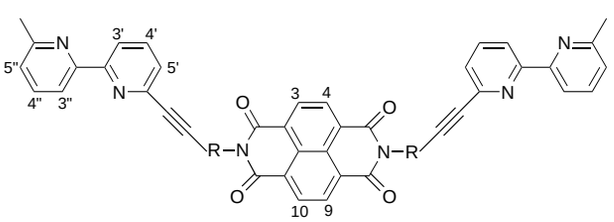

R

L^1 CH_2
L^2 CH_2CH_2
L^3 OCH_2

free amine during the coupling reaction. In support of this, under the same reaction conditions, treatment of propargyl alcohol **III** and but-3-ynyl alcohol **V** afforded the corresponding substituted bipyridines **VII** and **XI** respectively in modest reproducible yields (Scheme 2). Standard transformations of the alcohol functional group in bipyridyls **VII** and **XI** afforded the new substituted bipyridines **VII**–**X**, **XII** and **XIII**.

Ligands L^1 and L^2 were prepared as shown in Scheme 3, following a general procedure for the preparation of phthalate derivatives as precursors to the preparation of sensitive amines, *via* the azides.[8] Thus, treatment of azides **IX** and **XIII** with triphenylphosphine in toluene at reflux formed intermediate iminophosphoranes, which were trapped, *in situ*, with half an equivalent of the naphthalenetetracarboxylic dihydride **XIV** to give ligands L^1 and L^2 respectively. This reaction does not appear to have been widely applied to the preparation of aromatic diimides, which are generally prepared from the anhydride **XIV** and 2 equivalents of the amine.[9] Indeed, this was the original route used in the synthesis of L^1, by reaction of **XIV** with 2 equivalents of propargylamine **II** at high temperature.[5] The yields of this reaction were generally low and

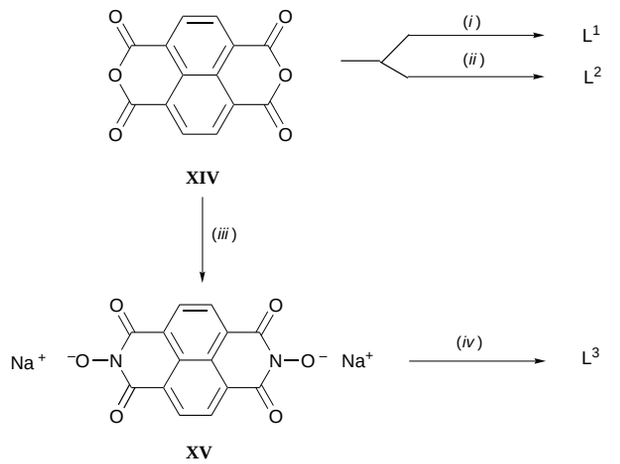

XIV

XV

Scheme 3 (*i*) PPh_3, NBu_4Cl; **IX**, PPh_3, NBu_4Cl; (*ii*) PPh_3, NBu_4Cl; **XIII**, PPh_3, NBu_4Cl; (*iii*) $NH_2OH{\cdot}HCl$, Na_2CO_3; (*iv*) **X**, dimethylformamide (dmf), 70–80 °C

isolation of the product difficult due to its low solubility. In addition, the synthesis of L^2 by the same route required the preparation of the amine **IV**, but despite several attempts the amine could not be isolated according to the literature procedure.[10]

Ligand L^3 was prepared from the same stock of starting materials. Thus, reaction of compound **XIV** with hydroxylamine under basic conditions afforded the disodium salt of *N*,*N*′-dihydroxynaphthalenetetracarboximide (Scheme 3).[11] Reaction of this salt with the bromobipyridine **X** gave L^3 in good yield. All three ligands L^1, L^2 and L^3 have poor solubility in most solvents and consequently purification to give analytically pure material was difficult, and satisfactory microanalytical data could not be obtained for L^2 and L^3. These ligands were characterised by mass and ^{1}H NMR spectra which were recorded on the protonated ligands in CF_3CO_2H–$CDCl_3$ and showed them to be >95% pure by integration.

Metal-ion complexation studies with L^1

The interaction of ligand L^1 with Zn^{II}, Cd^{II} and Cu^I, in the absence and presence of aromatic guest molecules, was studied.

***(a)* With zinc(II).** Preliminary metal-ion complexation studies of L^1 with Zn^{II} have been communicated previously.[5] Treatment of L^1 with 2.1 equivalents of zinc(II) triflate (trifluoromethanesulfonate) afforded complex **3**. Microanalysis of this complex was consistent with formation of $Zn_2L^1_2(SO_3CF_3)_4{\cdot}4H_2O$. In solution, at low concentration, or in the presence of an aromatic guest molecule S, this complex was assigned as the helical [2 + 2] metallomacrocycle.[5]

The formation of the supramolecular complexes $[Zn_2L^2{\cdot}S]^{4+}$, in which an aromatic substrate S is bound in the interior of the cavity (Scheme 1), is characterised by a colour change due to charge transfer between the electron-deficient pyromellitimide spacers and the bound substrate. Deep red single crystals suitable for examination by X-ray diffraction were isolated by infusion of diisopropyl ether into an acetonitrile solution of ligand L^1 (4 mmol dm^{-1}), zinc triflate (4 mmol dm^{-1}) and 1 equivalent of either *p*- or *o*-dimethoxybenzene to give complexes **1** and **2** respectively (Table 1). The crystals of each complex were extremely volatile, and the quality of the diffraction data was significantly compromised by severe substrate, solvate and counter ion disorder in the lattice. Similar problems in obtaining high-quality data have been reported by Fujita *et al.*[12] in attempts to characterise molecular boxes assembled from 4,4′-bipyridyl and palladium(II), and Stang and co-workers[13] in the characterisation of iodonium transition-metal tetranuclear macrocyclic squares; disordered triflates as well as solvent of

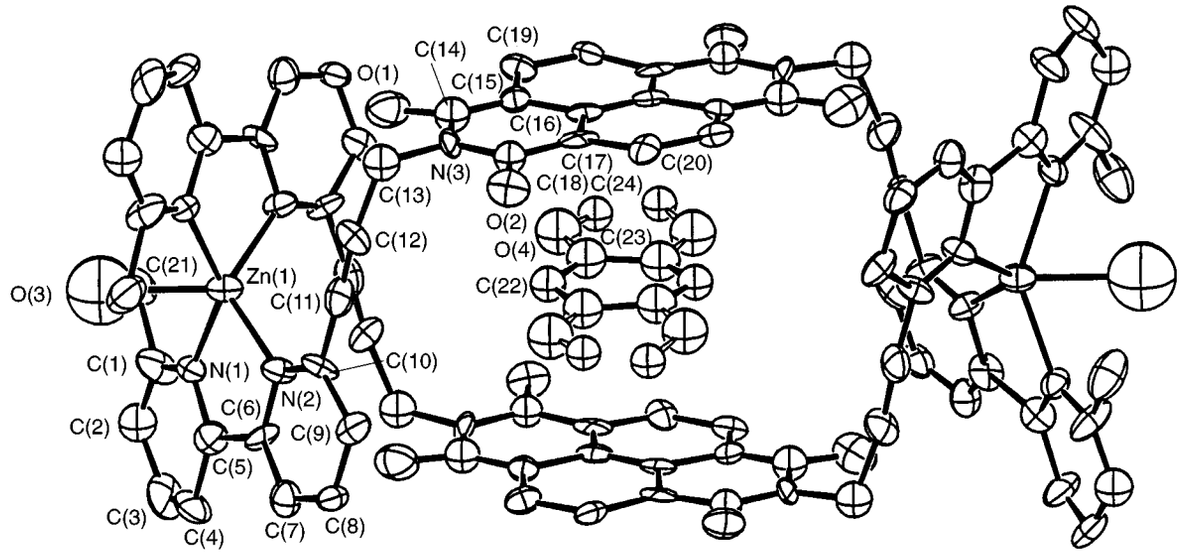

Fig. 1 An ORTEP projection of complex **1** with 15% displacement envelopes. The Zn–Zn principal axis of the complex resides on a two-fold axis of the space group *Cccm*, and a two-fold axis also passes orthogonally through the centre of the pyromellitimide bridge. The substrate is disordered about two rotationally related orientations

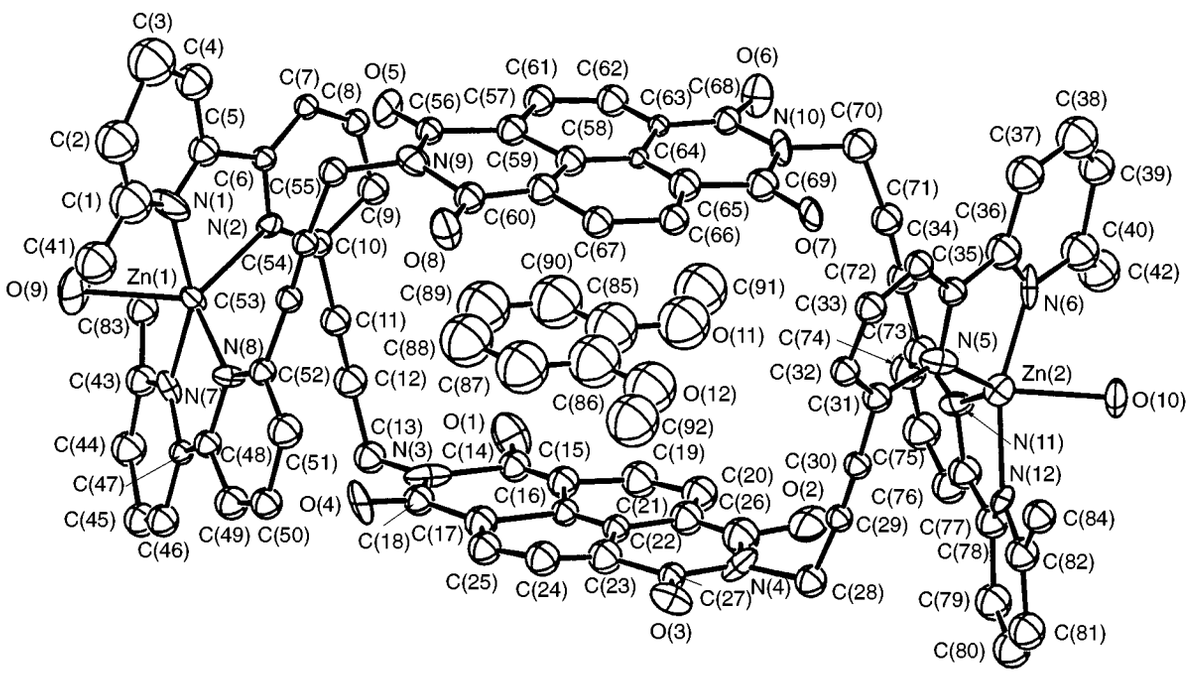

Fig. 2 An ORTEP projection of complex **2** with 15% displacement envelopes

crystallisation that was lost on mounting of the crystals precluded satisfactory crystallographic analysis in several cases.[13]

Figs. 1 and 2 show ORTEP[14] depictions of the two complexes which reveal the presence of the chiral [2 + 2] metallomacrocycle with a substrate molecule bound in the interior of the cavity. In the case of complex **1**, the bound *p*-dimethoxybenzene is disordered about two rotationally related orientations. The structure (Fig. 1) contains alternating layers of complex and substrate and counter ion stacked in the *c* direction. Interleaved π stacking of the complexes and substrate in columns at 0,0,*z*, and $\frac{1}{2},\frac{1}{2},z$ provides large channels centred on $\frac{1}{2},0,z$, $0,\frac{1}{2},z$, $\frac{1}{2},1,z$ and $1,\frac{1}{2},z$. These channels presumably facilitate the escape of solvent and substrate molecules from the lattice. The structure of complex **2** (Fig. 2) has alternating layers of complex and substrate stacked in the *b* direction. However in contrast to **1**, the π-stacking planes are orthogonal to the *bc* diagonal, *i.e.* the structure contains columns of interleaved complex and substrate aligned in the *bc* diagonal direction. The columns are surrounded by triflate counter ions.

Figs. 3 and 4 depict the orientation of the substrates with respect to the pyromellitimide spacers and highlight the impact of the substrate on the shape of the cavities in the metallomacrocycles. In both cases, the offset stacked geometry of the substrates with respect to the pyromellitimide spacers is apparent. However, the positioning of each of the bound substrates with respect to the central naphthalene portion of the pyromellitimide spacer is different, as are the relative positions of the two pyromellitimide rings in each complex. Undoubtedly these differences reflect a substrate-dependent balance between an optimum π-stacking interaction and the minimisation of electrostatic repulsions associated with close contact between the substrate and host atoms. Such π-stacking interactions have been observed in organic host–guest systems including molecular clefts and macrocyclic complexes.[15]

A comparison of structures **1** and **2** reveals several significant differences (Table 1). The *o*-dimethoxybenzene substrate has a greater effective width than *p*-dimethoxybenzene. Accordingly there is a reduction of the pyromellitimide–pyromellitimide

Table 1 Selected bond lengths (Å) and angles (°) for complexes **1** and **2**

Complex **1**

Zn(1)–O(3)	2.27(7)	Zn(1)–N(2)	2.03(3)
Zn(1)–N(1)	2.04(2)		
O(3)–Zn(1)–N(1)	70.9(7)	N(1")–Zn(1)–N(2")	114(1)
O(3)–Zn(1)–N(2)	119.7(8)	Zn(1)–N(1)–C(1)	132(3)
N(1)–Zn(1)–N(2)	114(1)	Zn(1)–N(1)–C(5)	108(2)
N(1)–Zn(1)–N(1")	142(1)	C(1)–N(1)–C(5)	120(3)
N(1)–Zn(1)–N(2")	85(1)	Zn(1)–N(2)–C(6)	112(2)
N(2)–Zn(1)–N(1")	85(1)	Zn(1)–N(2)–C(10)	19(2)
N(2)–Zn(1)–N(2")	121(1)		

Complex **2**

Zn(1)–O(9)	2.20(4)	Zn(2)–O(10)	2.18(4)
Zn(1)–N(1)	2.00(4)	Zn(2)–N(5)	1.96(4)
Zn(1)–N(2)	2.13(3)	Zn(2)–N(6)	1.96(4)
Zn(1)–N(7)	2.08(3)	Zn(2)–N(11)	1.99(3)
Zn(1)–N(8)	1.96(3)	Zn(2)–N(12)	2.03(3)
O(9)–Zn(1)–N(1)	77(2)	N(6)–Zn(2)–N(12)	161(2)
O(9)–Zn(1)–N(2)	126(1)	N(11)–Zn(2)–N(12)	78(1)
O(9)–Zn(1)–N(7)	79(2)	Zn(1)–N(1)–C(1)	125(4)
O(9)–Zn(1)–N(8)	116(1)	Zn(1)–N(1)–C(5)	113(4)
N(1)–Zn(1)–N(2)	80(2)	Zn(1)–N(2)–C(6)	112(3)
N(1)–Zn(1)–N(7)	155(2)	Zn(1)–N(2)–C(10)	127(3)
N(1)–Zn(1)–N(8)	113(2)	Zn(2)–N(5)–C(31)	133(3)
N(2)–Zn(1)–N(7)	112(1)	Zn(2)–N(5)–C(35)	116(3)
N(2)–Zn(1)–N(8)	119(1)	Zn(2)–N(6)–C(36)	113(4)
N(7)–Zn(1)–N(8)	82(1)	Zn(2)–N(6)–C(40)	126(4)
O(10)–Zn(2)–N(5)	123(1)	Zn(1)–N(7)–C(43)	123(3)
O(10)–Zn(2)–N(6)	78(2)	Zn(1)–N(7)–C(47)	110(3)
O(10)–Zn(2)–N(11)	116(1)	Zn(1)–N(8)–C(48)	108(2)
O(10)–Zn(2)–N(12)	84(1)	Zn(1)–N(8)–C(52)	130(3)
N(5)–Zn(2)–N(6)	82(2)	Zn(2)–N(11)–C(73)	127(3)
N(5)–Zn(2)–N(11)	121(1)	Zn(2)–N(11)–C(77)	121(3)
N(5)–Zn(2)–N(12)	112(1)	Zn(2)–N(12)–C(78)	113(3)
N(6)–Zn(2)–N(11)	106(1)	Zn(2)–N(12)–C(82)	127(3)

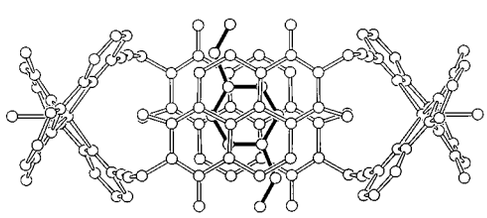

Fig. 3 A ball and stick depiction of complex **1** indicating the disposition of the bound *p*-dimethoxybenzene (black) with respect to the pyromellitimide spacers. Only one of the two orientations of the substrate is shown (see Fig. 2).

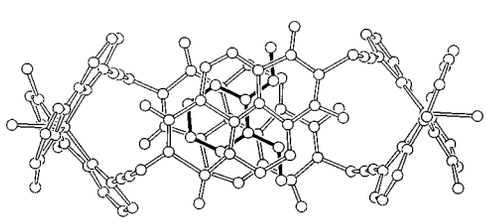

Fig. 4 A ball and stick depiction of complex **2** indicating the disposition of the bound *o*-dimethoxybenzene (black) with respect to the pyromellitimide spacers

crossover angle from 61° in complex **1** to 51° in **2**, and a concomitant increase in the Zn to Zn distance from 14.5 Å in **1** to 15.1 Å in complex **2**. The separation between the substrate and the pyromellitimide backbones is comparable in both complexes. Both complexes have distorted trigonal-bipyramidal coordination spheres, with axially co-ordinated water molecules 2.27(7) Å from the zinc in complex **1** and 2.20(4) Å and 2.18(4) Å from zinc in **2**. The very large thermal envelope of the site refined as co-ordinated water in complex **1** suggests that it may not be fully occupied. The poor quality of the diffraction data did not permit an unambiguous refinement of the site occupancy.

While the crystal structures of complexes **1** and **2** provide clear evidence for substrate binding in the solid state, independent evidence for the inclusion of a guest molecule in the cavity in solution was obtained from NMR studies. A simple NMR assay was developed which allowed rapid screening of substrates for their potential to bind in the cavity. The pyromellitimide rings, in the absence of a guest molecule, are rapidly rotating on the NMR time-scale and hence H[3,4,9,10] appear as a sharp singlet.[5] Addition of a guest molecule which binds in the cavity hinders the aryl ring rotation, as the included guest molecule must be displaced to allow free rotation.[5] Hence, broadening of the pyromellitimide protons H,[3,4,9,10] at room temperature, on addition of an aromatic substrate, was taken as evidence for binding of the substrate in the cavity of the metallomacrocycle.

We have previously reported that anisole, *o*-, *m*- and *p*-dimethoxybenzene as well as nitrobenzene bind weakly in the cavity presumably by favourable electrostatic interactions with the aromatic spacers.[5] Some discrimination between the isomers of dimethoxybenzene was observed with *p*-dimethoxybenzene binding more weakly than the *ortho* and *meta* isomers.

The ability of a range of electon-rich aromatic substrates to bind to the metallomacrocycle $[Zn_2L^1_2]^{4+}$ was further examined in a series of titration experiments carried out by adding 1.0 equivalent of benzene, naphthalene, 3,5-dimethoxybenzyl alcohol, phenol, resorcinol, 1,6-dimethoxynaphthalene and 1,6-dihydroxynaphthalene to a solution of the zinc(II) metallomacrocycle. In each case a colour change (generally yellow to red) was observed on addition of the aromatic substrate, and the pyromellitimide resonance broadened. These results are entirely consistent with formation of a charge-transfer complex between the electron-rich aromatic substrate binding between the electron-poor pyromellitimide spacers (Scheme 1). Attempts to bind chiral aromatic substrates (*e.g.* aromatic amino acids), in order to see whether preferential stabilisation of one of the helical enantiomers was observed, were hampered by poor solubility of the substrates in acetonitrile. An attempt to resolve racemic 1,1′-binaphthol or the dimethyl derivative were unsuccessful and no evidence for binding of either enantiomer was observed, presumably due to steric interactions. Further studies in this area will require the development of metallomacrocycles which are stable in polar solvents and water.

***(b)* With copper(I).** Microanalysis of the brick red copper(I) complex isolated from treatment of ligand L^1 and an equimolar amount of copper(I) chloride, followed by addition of ammonium hexafluorophosphate, was consistent with formation of the hydrate $Cu_2L^1_2(PF_6)_2 \cdot H_2O$ **4**. However, in contrast to the corresponding zinc(II) complex **3**, the ^{1}H NMR spectra of **4** in either CD_3CN or CD_2Cl_2 showed only severely broadened resonances at a range of concentrations [*e.g.* Fig. 5(*a*)].

The copper(I) L^1 complex **4** was shown to be capable of substrate recognition, in a similar manner to that observed for the zinc complex **3**. In CD_3CN the NMR spectrum of **4** contained only broad signals [Fig. 5(*a*)] consistent with an equilibrium between multiple complexes (Scheme 4) and/or solvent exchange on the ^{1}H NMR time-scale. When an excess of *m*-dimethoxybenzene was added to this solution the ^{1}H NMR spectrum sharpened [Fig. 5(*b*), 5(*c*)]. After the addition of 24 equivalents of substrate, sharp signals which were fully assigned to only one [2 + 2] metallomacrocycle were observed [Fig. 5(*c*)]. The chemical shifts and appearance of the aromatic protons were comparable to those of the corresponding zinc(II) complex **3** suggesting that the copper(I) and zinc(II) complexes are struc-

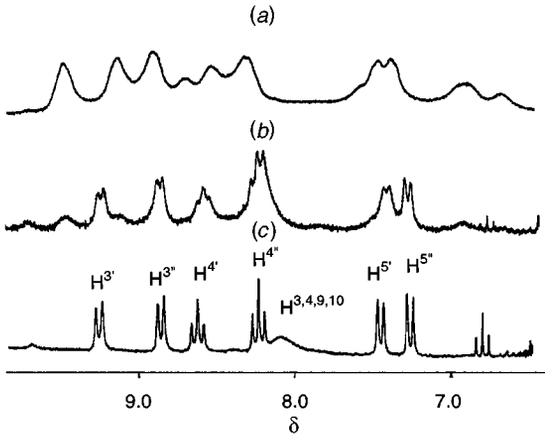

Fig. 5 The 400 MHz ^{1}H NMR spectra at 300 K of the copper(I)–L^1 complex **4** in CD_3CN (*a*) and after the addition of 3 (*b*) and 24 equivalents *m*-methoxybenzene

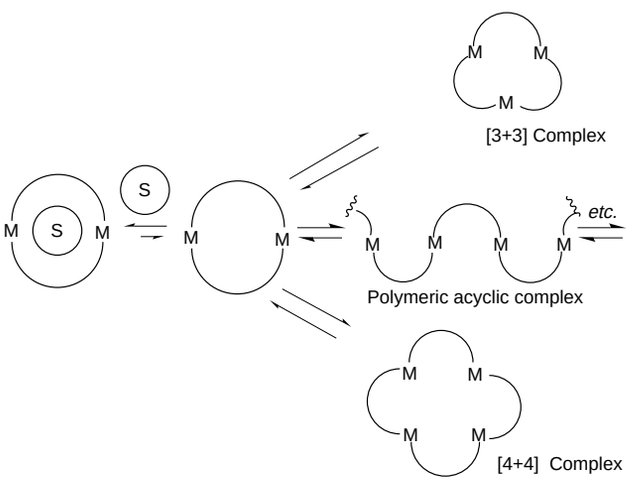

Scheme 4 Representation of the equilibration observed between L^1 and Zn^{II} or Cu^I in the presence and absence of aromatic substrate leading to exclusive formation of the chiral, helical [2 + 2] metallomacrocycle; the stereochemical at metal centres in solution may be four- or five-co-ordinate

turally similar. As was the case for **3**, the pyromellitimide protons $H^{3,4,9,10}$ in the copper(I) complex **4** appeared as a broad signal [δ 8.1, Fig. 5(*c*)] consistent with restricted rotation of the aromatic rings on the NMR time-scale as a result of inclusion of *m*-dimethoxybenzene in the cavity of the metallomacrocycle. This is the only example of a copper(I) complex prepared from a variety of bis(bipyridyl) ligands,[4] which exists as a single species in solution irrespective of solvent or solution concentration. The second-sphere co-ordination of the electron-rich substrate *m*-dimethoxybenzene changes the equilibrium to favour a single product *via* a selective recognition process. Furthermore, exchange with the co-ordinating solvent CD_3CN is almost negligible and emphasises the particular stability of the receptor–substrate complex.

Formation of the supramolecular copper(I) complex **4** required a significantly higher number of equivalents (>20) of aromatic substrate compared with the corresponding zinc(II) complex **3**, in which the same effect was observed in the presence of <3 equivalents of substrate. This result is most probably a result of the stricter stereochemical requirement of copper(I) complexes to adopt a tetrahedral geometry with 6,6-disubstituted bipyridyls, which gives a more strained metallomacrocycle, compared with zinc(II) which can readily adopt a range of co-ordination geometries with substituted 2,2′-bipyridyls.

(*c*) With cadmium(II). Given the similar co-ordination chemistry exhibited by zinc(II) and cadmium(II), it was expected that ligand L^1 would form structurally similar supramolecular complexes with both zinc(II) and cadmium(II). Treatment of L^1 with cadmium triflate under identical conditions to those used to form zinc(II) complex **3** afforded the cadmium complex **5**. The ^{1}H NMR spectrum of this complex in CD_3CN (3.7 mM) showed the presence of one major complex, with all resonances at similar chemical shifts to those found for the corresponding zinc complex **3**. In particular in the methylene region of the spectrum an AX system was observed which was assigned to the helical complex on comparison with the chemical shifts observed for these protons in the helical isomer of the zinc(II) complex. Minor peaks (<10%) were also observed in this region of the spectrum at higher sample concentrations. While detailed studies were not carried out on the cadmium complex, the NMR studies are consistent with formation of the chiral [2 + 2] metallomacrocycle.

Metal-ion-complexation studies with L^2 and L^3

The results obtained with ligand L^1 and both zinc(II) and copper(I) suggested that the desired [2 + 2] metallomacrocycles were strained, and hence required the additional stacking interaction of a bound aromatic substrate to stabilise the [2 + 2] complex (Scheme 4). This was further emphasised by the distorted geometries at the metal centres in the crystal structures of the zinc(II) complexes **1** and **2**. Ligands L^2 and L^3, which contain an additional carbon and oxygen atom respectively in the linkers separating the bipyridyl groups from the aromatic spacer, were prepared in order to assess whether the additional atoms in the linker would allow formation of stable [2 + 2] metallomacrocycles in the absence of guest molecules.

Zinc(II) complexes were prepared with ligands L^2 and L^3 in an analogous manner to the zinc(II) complex of L^1, **3**. However, in CD_3CN solution, only broadened NMR spectra were obtained with both complexes. These spectra failed to sharpen in the presence of mono- or di-substituted aromatics. These results are consistent with the formation of equilibrating oligomers of complexes in solution and highlight the crucial role served by the three-atom linker in ligand L^1 in the assembly of the helical metallomacrocycle. While the linkers present in L^2 and L^3 are slightly longer than that in L^1, and hence may allow a more regular co-ordination geometry at the metal centres to be achieved, the additional atom in each case also increases the rotational degrees of freedom in the ligands and hence the probability of forming oligomeric complexes.

Conclusion

The two crystal structures reported, while of limited quality, nevertheless confirm our previous NMR assignment of the stereochemistry of the chiral [2 + 2] metallomacrocycle, and illustrate the important advantages of metallomacrocycles in the study of molecular recognition. The 2,2′-bipyridyl co-ordination sites are important features of the structures that provide a mechanism whereby the dimensions of the cavity may be altered to accommodate optimum binding of aromatic substrates. The substrate effectively templates or selects its optimum metallomacrocycle host from the range of geometries and oligomers present in solutions of ligand L^1 and zinc(II). The low stereochemical preference of zinc(II) is probably important in this particular system, as it allows a range of co-ordination geometries, and hence metallomacrocycles of different shapes and dimensions, to be assembled.

The contrasting results obtained with L^1 compared to L^2 and L^3 highlight the importance of the rigid propargyl linker in directing the outcome of the assembly process. The rigidity of this linker serves two important roles. First, direct substitution of the acetylene portion of the linker at the 6′-position of the bipyridyl orients the pyromellitimide spacer in a manner which

favours formation of the helical rather than the non-helical isomer. Secondly, the restricted rotation in the linker also promotes formation of the [2 + 2] metallomacrocycle rather than other oligomeric complexes in solution. Incorporation of the acetylene-substituted bipyridyl unit into new ligands should allow the development of multicomponent supramolecular structures involving more than two metal ions.

Experimental

Tetrahydrofuran was dried over sodium–benzophenone and distilled prior to use. Melting points were determined on a Reichert heating stage and are uncorrected. Proton NMR spectra were recorded at 200 MHz on a Bruker AC200F instrument, in the solvent indicated and referenced to the residual solvent proton signal. Microanalyses were performed by the Microanalytical Unit at The University of New South Wales. Electron-impact (EI) and high-resolution (HR) mass spectra were recorded on a Kratos MS50 instrument. Matrix-assisted laser desorption ionisation (MALDI) mass spectra were recorded on a VG TofSpec instrument using sinapinic (3,5-dimethoxy-4-hydroxycinnamic acid) as matrix. Chromatography was carried out on Merck type 9385 silica gel.

Preparations

6-Bromo-6′-methyl-2,2′-bipyridine I. 2-Methyl-6-trimethylstannylpyridine[6] (16.1 g, 62.8 mmol), 2,6-dibromopyridine (13.9 g, 62.8 mmol) and $[Pd(PPh_3)_2Cl_2]$ (2.20 g, 3.14 mmol) were dissolved in thf (600 cm^3) and the mixture was heated at reflux for 15 h. The mixture was cooled and the solvent removed by rotary evaporation under reduced pressure. The crude yellow residue was recrystallised from light petroleum (b.p. 40–60 °C) to give a white solid (9.7 g) which was purified by chromatography (20% ethyl acetate–heptane) to give compound **I** as a white solid (6.8 g, 44%), m.p. 111 °C (Found: C, 53.4; H, 3.4; N, 11.0. $C_{11}H_9BrN_2$ requires C, 53.0; H, 3.6; N, 11.2%). ^{1}H NMR ($CDCl_3$): δ 2.62 (s, CH_3), 7.18 (d, *J* 7.8, $H^{5'}$), 7.46 (d, *J* 7.9 H^5), 7.65 and 7.70 (2dd, *J* 7.8, 7.8, H^4 and $H^{4'}$), 8.19 (d, *J* 7.8, $H^{3'}$) and 8.41 (d, *J* 7.8 Hz, H^3). EI mass spectrum: *m*/*z* 250 [M^+ (^{81}Br), 60], 248 [M^+ (^{79}Br), 62], 169 (100), 156 (65), 141 (23), 128 (36), 92 (28), 69 (27), 65 (28) and 43 (52%). A later fraction contained 6.6″-dimethyl-2,2′:6′,2″-terpyridine (1.05 g, 20%), a portion of which was recrystallised from light petroleum to give terpyridine as white needles, with EI mass and ^{1}H NMR spectra consistent with those reported,[16] mp 173–174 °C (lit.,[16] 158–161 °C).

4-Hydroxy-1-(6′-methyl-2,2′-bipyridin-6-yl)but-1-yne XI. Compound **I** (2.0 g, 8.10 mmol), $[Pd(PPh_3)_4]$ (0.47 g, 0.040 mmol) and CuI (150 mg, 0.08 mmol), were mixed in a dry flask under argon. Tetrahydrofuran (50 cm^3) was added, followed by but-3-ynyl alcohol (1.24 cm^3, 1.15 g, 16.2 mmol) and diisopropylamine (10 cm^3). The mixture was stirred at reflux under argon for 5 h. The mixture was then cooled, poured into a solution of KCN (1.0 g) in water (50 cm^3) and extracted with chloroform (3 × 50 cm^3). The extracts were washed with water and then NaCl and dried over Na_2SO_4. The solvent was removed under reduced pressure to give an oil which was chromatographed using 50% ethyl acetate–light petroleum as eluent to give compound **XI** as a white solid (1.33 g, 54%). A small amount was recrystallised from light petroleum as colourless plates, m.p. 97–99 °C (Found: C, 75.8; H, 6.16; N, 11.5. $C_{15}H_{14}N_2O$ requires C, 75.6; H, 5.92; N, 11.7%). ^{1}H NMR ($CDCl_3$): δ 2.65 (s, CH_3), 2.73 (dd, *J* 6.2, 6.2, H^3), 2.93 (br s, OH), 3.86 (dd, *J* 6.3, 6.3, H^4), 7.19 (d, *J* 7.6, $H^{5''}$), 7.40 (dd, *J* 7.8, 0.7, $H^{5'}$), 7.72 and 7.75 (2dd, *J* 7.6, 7.6, $H^{4'}$ and $H^{4''}$), 8.21 (d, *J* 7.8, $H^{3''}$) and 8.38 (dd, *J* 7.9, 0.7 Hz, $H^{3'}$). EI mass spectrum: *m*/*z* 238 (M^+, 27), 221 (4), 209 (49), 208 (100), 207 (44), 206 (34), 192 (16), 178 (5), 165 (4) and 142 (7%).

3-Hydroxy-1-(6′-methyl-2′,2″-bipyridin-6-yl)prop-1-yne VII. Using the above procedure compound **VII** was prepared as a white solid (67%), mp 106 °C (Found: C, 74.7; H, 5.6; N, 12.4. $C_{14}H_{12}N_2O$ requires C, 75.0; H, 5.4; N, 12.5%). ^{1}H NMR ($CDCl_3$): δ 2.38 (br s, OH), 2.64 (s, CH_3), 4.56 (s, H^2), 7.18 (d, *J* 7.7, $H^{5''}$), 7.43 (dd, *J* 7.5, 1.0, $H^{5'}$), 7.69 and 7.78 (2dd, *J* 7.7, $H^{4'}$ and $H^{4''}$), 8.20 (d, *J* 7.7, $H^{3''}$) and 8.39 (dd, *J* 7.5, 1.0 Hz, $H^{3'}$). EI mass spectrum: *m*/*z* 224 (M^+, 64), 196 (17), 195 (100), 170 (12) and 169 (13%).

4-Azido-1-(6′-methyl-2,2′-bipyridin-6-yl)but-1-yne XIII. Methanesulfonyl chloride (0.45 cm^3) was added slowly to a stirred ice-cooled solution of the alcohol **XI** (1.20 g, 4.65 mmol) and triethylamine (0.75 cm^3) in dry diethyl ether (100 cm^3) and the resulting mixture was stirred at room temperature (r.t.) for 2 h. The mixture was poured into water (100 cm^3) and extracted with ethyl acetate (3 × 50 cm^3).The extracts were washed with water and NaCl and dried over Na_2SO_4. The solvent was removed to give the crude mesylate, **XII**, as a white solid (1.58 g, 100%) which was used in the next step without further purification. A small amount was recrystallised from light petroleum as colourless needles, m.p. 88–90 °C. ^{1}H NMR ($CDCl_3$): δ 2.62 (s, CH_3), 2.96 (dd, *J* 6.7, 6.7, H^3), 3.11 (s, OSO_2CH_3), 4.52 (dd, *J* 6.7, 6.7, H^4), 7.18 (d, *J* 7.6, $H^{5''}$), 7.40 (dd, *J* 7.8, 0.7, $H^{5'}$), 7.69 and 7.76 (2dd, *J* 7.6, 7.6, $H^{4'}$ and $H^{4''}$), 8.19 (d, *J* 7.8, $H^{3''}$) and 8.38 (dd, *J* 7.9, 0.7 Hz, $H^{3''}$).

The crude mesylate **XII** (0.90 g, 2.85 mmol) and NaN_3 (0.50 g, 7.77 mmol) were mixed in dmf (70 cm^3) and the mixture was stirred at 65 °C for 4 h. The mixture was cooled, poured into water (100 cm^3) and extracted with chloroform (3 × 70 cm^3). The extracts were washed with water and NaCl, dried over Na_2SO_4 and the solvent was removed by rotary evaporation to give a tan semi-solid. The crude product was chromatographed eluting with 20% ethyl acetate–heptane to give compound **XIII** as a white solid (0.66 g, 88% overall from **XI**). A small amount was recrystallised from light petroleum as colourless plates, m.p. 63–65 °C (Found: C, 68.5; H, 5.03; N, 26.4. $C_{15}H_{13}N_5$ requires C, 68.4; H, 4.98; N, 26.6%). ^{1}H NMR ($CDCl_3$): δ 2.65 (s, CH_3), 2.77 (dd, *J* 6.9, 6.9, H^3), 3.54 (dd, *J* 6.9, 6.9, H^4), 7.18 (d, *J* 7.6, $H^{5''}$), 7.42 (d, *J* 7.7, $H^{5'}$), 7.71 and 7.76 (2dd, *J* 7.7, 7.7, $H^{4'}$ and $H^{4''}$), 8.24 (d, *J* 7.8, $H^{3''}$) and 8.42 (d, *J* 7.9 Hz, $H^{3'}$). EI mass spectrum: *m*/*z* 263 (M^+, 65), 235 (31), 234 (32), 220 (14), 208 (85), 207 (100), 206 (50), 193 (29), 165 (10) and 142 (10%).

3-Azido-1-(6′-methyl-2,2′-bipyridin-6-yl)prop-1-yne IX. Using the above procedure, the alcohol **VII** (1.22 g, 5.5 mmol) was converted initially into mesylate **VIII** which was chromatographed, eluting with 30% ethyl acetate–heptane, as a white solid (1.54 g, 94%). A small amount was recrystallised from light petroleum as colourless plates, m.p. 98–100 °C. ^{1}H NMR ($CDCl_3$): δ 2.62 (s, CH_3), 3.22 (s, OSO_2CH_3), 5.13 (s, H^3), 7.19 (d, *J* 7.6, $H^{5''}$), 7.47 (dd, *J* 7.7, 0.9, $H^{5'}$), 7.70 and 7.80 (2 dd, *J* 7.8, 7.8, $H^{4'}$ and $H^{4''}$), 8.28 (d, *J* 7.8, $H^{3''}$) and 8.45 (dd, *J* 8.2, 0.9 Hz, $H^{3'}$). The mesylate **VIII** (1.0 g, 3.31 mmol) was converted into azide **IX** which was purified by chromatography over silica (30% ethyl acetate–heptane) as a white solid (0.58 g, 66% from **VII**), m.p. 83–87 °C (Found: *m*/*z* 249.1010. Calc. for $C_{14}H_{11}N_5$: *m*/*z* 249.1014). ^{1}H NMR ($CDCl_3$): δ 2.63 (s, CH_3), 4.21 (s, H^3), 7.18 (d, *J* 7.7, $H^{5''}$), 7.48 (dd, *J* 7.7, 1.1, $H^{5'}$), 7.70 and 7.79 (2dd, *J* 7.8, 7.8, $H^{4'}$ and $H^{4''}$), 8.22 (d, *J* 7.8, $H^{3''}$) and 8.42 (dd, *J* 8.1, 0.9 Hz, $H^{3'}$). EI mass spectrum: *m*/*z* 249 (M^+, 65), 221 (45), 220 (78), 208 (80), 207 (48),195 (48), 181 (20), 179 (18), 169 (25), 131 (23) and 69 (68%).

3-Bromo-1-(6′-methyl-2,2′-bipyridin-6-yl)prop-1-yne X. The mesylate **VIII** (1.04 g, 3.45 mmol) was dissolved in dmf (50 cm^3), LiBr (0.74 g, 8.63 mmol) added and the mixture stirred under nitrogen at r.t. for 2 h. Water (100 cm^3) was added and the resulting precipitate collected and air-dried. Purification by

chromatography over silica ($CHCl_3$–heptane 1:1) afforded the bromide **X** as a beige solid (0.73 g, 74%). A small portion was recrystallised from light petroleum as white needles, m.p. 114 °C (Found: C, 58.8; H, 4.0; N, 9.3. $C_{14}H_{11}BrN_2$ requires C, 58.6; H, 3.9; N, 9.8%). ^{1}H NMR ($CDCl_3$): δ 2.64 (s, CH_3), 4.19 (s, H^3), 7.19 (d, *J* 7.6, $H^{5''}$), 7.46 (dd, *J* 7.5, 1.0, $H^{5'}$), 7.71 and 7.78 (2dd, *J* 7.6, 7.6, $H^{4'}$ and $H^{4''}$), 8.22 (d, *J* 7.6, $H^{3''}$) and 8.43 (dd, *J* 7.5, 1.0 Hz, $H^{3'}$). EI mass spectrum: *m*/*z* 288 [M^+ (^{81}Br), 23], 286 [M^+ (^{79}Br), 23], 208 (21), 207 (100), 206 (22), 205 (20), 192 (10), 178 (8), 150 (6) and 103 (14%).

***N*,*N*′-Bis[4-(6′-methyl-2,2′-bipyridin-6-yl)but-3-ynyl]-naphthalene-1,8:4,5-tetracarboximide L^2**. Azide **XIII** (300 mg, 1.14 mmol) and naphthalene-1,8:4,5-tetracarboxylic anhydride (150 mg, 0.57 mmol) were mixed in toluene (45 cm^3) under argon. Tetrabutylammonium bromide (45 mg) and triphenylphosphine (330 mg, 1.25 mmol) were added and the mixture was stirred under argon at reflux for 4 h. The mixture was cooled and poured into ether (100 cm^3) forming a beige precipitate. The precipitate was collected (315 mg) and washed with chloroform to give L^2 as a yellow powder (170 mg), m.p. >300 °C. The filtrate was slowly reduced precipitating a second crop of product (60 mg; total yield 230 mg, 61%). ^{1}H NMR ($CDCl_3$–CF_3CO_2H): δ 2.96 (s, CH_3), 3.05 and 4.59 (2 dd, *J* 6.6, 6.6, CH_2CH_2), 7.62 (dd, *J* 7.4, 1.0, $H^{5''}$) 7.79 (d, *J* 7.8, $H^{5'}$), 7.98 (dd, *J* 7.9, 7.9, $H^{4''}$), 8.06 (dd, *J* 7.9, 1.0, $H^{3''}$), 8.27 (d, *J* 7.8, $H^{3'}$), 8.49 (dd, *J* 8.0, 8.0, $H^{4'}$) and 8.52 (s, $H^{3,4,9,10}$). MALDI mass spectrum: *m*/*z* 707.2 (M^+ + 1, 707.2). EI mass spectrum: *m*/*z* 502 (18), 501 (45), 499 (11), 473 (2), 446 (16), 445 (7), 368 (12), 289 (18), 265 (18), 131 (45), 100 (63) and 81 (100%).

***N*,*N*′-Bis[3-(6′-methyl-2,2′-bipyridin-6-yl)prop-2-ynyl]-naphthalene-1,8:4,5-tetracarboximide L^1**. Using the procedure outlined above for the synthesis of L^2, L^1 was prepared as a yellow powder (51%), m.p. >300 °C (Found: C, 73.0; H, 4.2; N, 11.8. $C_{42}H_{26}N_6O_4\cdot 0.5H_2O$ requires C, 73.3; H, 4.0; N, 12.2%). ^{1}H NMR ($CDCl_3$–CF_3CO_2D): δ 2.91 (s, CH_3), 5.30 (s, CH_2), 7.73 (dd, *J* 7.3, 1.1 Hz, $H^{5''}$), 7.80 (d, *J* 8.0, $H^{5'}$), 8.00 (dd, *J* 7.9, 7.9, $H^{4''}$), 8.07 (dd, *J* 6.9, 0.9, $H^{3''}$), 8.28 (d, *J* 8.1, $H^{3'}$), 8.49 (dd, *J* 7.9, 7.9 Hz, $H^{4'}$) and 8.90 (s, $H^{3,4,9,10}$). EI mass spectrum: *m*/*z* 678 (M^+, 57), 472 (94), 226 (43), 207 (37), 184 (100), 169 (40) and 28 (45%).

***N*,*N*′-Bis[3-(6′-methyl-2,2′-bipyridin-6-yl)prop-2-ynyloxy]-naphthalene-1,8:4,5-tetracarboximide L^3**. Following the method of Zhong *et al.*[11] naphthalene-1,8:4,5-tetracarboxylic dianhydride (1.0 g, 3.73 mmol), sodium carbonate (1.64 g) and hydroxylamine hydrochloride (1.31 g) were mixed in water (30 cm^3), the mixture was heated at 80 °C for 30 min and then at 110 °C for 1 h. After cooling to room temperature, the precipitate was collected, washed with warm water (100 cm^3), and dried under vacuum to give the disodium salt of *N*,*N*′-dihydroxynaphthalene-1,8:4,5-tetracarboximide **XV** as a purple powder (0.9 g, 71%) which was used directly in the next step. The salt **XV** (50 mg, 0.146 mmol) and **X** (110 mg, 0.38 mmol) were mixed in dmf (15 cm^3) and the mixture was stirred under argon at 70–80 °C for 3 h. It was cooled to room temperature and the resulting precipitate collected, washed with water and ethanol to give L^3 as a beige powder (95 mg, 93%), m.p. 270 °C (decomp.). ^{1}H NMR ($CDCl_3$–CF_3CO_2H): δ 2.92 (s, CH_3), 5.27 (s, CH_2), 7.63 (dd, *J* 7.8, 0.9, $H^{5''}$), 7.81 (d, *J* 7.8, $H^{5'}$), 7.93 (dd, *J* 7.9, 7.9, $H^{4''}$), 8.03 (dd, *J* 7.9, 0.9, $H^{3''}$), 8.26 (d, *J* 8.1, $H^{3'}$), 8.46 (dd, *J* 7.9, 7.9 Hz, $H^{4'}$) and 8.82 (s, $H^{3,4,9,10}$). MALDI mass spectrum: *m*/*z* 711.1 (M^+ + 1, 711.2). EI mass spectrum: *m*/*z* 338 (1), 226 (24), 222 (100), 207 (114), 194 (68), 179 (20), 170 (24) and 152 (14%).

Reactions of ligand L^1.

With CuCl. Ligand L^1 (20 mg, 35 mmol) was added to a solution of copper(I) chloride (16 mg, 160 mmol) and hydrazine hydrate (1 cm^3) in MeCN–water (2:3, 5 cm^3). The mixture was stirred at room temperature for 3 h and ammonium hexafluorophosphate (100 mg, 610 mmol) in water (2 cm^3) was added. The resultant red precipitate was collected, washed successively with water (10 cm^3) and $CHCl_3$ (10 cm^3) and dried under high vacuum to give the complex $Cu_2L^1{}_2(PF_6)_2\cdot 2H_2O$ **4** as a red solid (22 mg, 81%) (Found: C, 56.3; H, 3.4; N, 9.1. $C_{84}H_{54}Cu_2F_{12}N_{12}O_9P_2$ requires C, 56.2; H, 3.0; N, 9.3%). ^{1}H NMR (400 MHz, CD_2Cl_2): δ 1.2–1.9 (br s), 3.5–4.7 (br m) and 6.9–9.5 (br m). λ_{max}(log ε) (MeCN) 232 (5.28), 296 (4.75) and 322 (4.25) nm. ES mass spectrum: *m*/*z* 742 ($M - 2PF_6^-$) and 679 (HL^{1+}).

With Zn(CF$_3$SO$_3$)$_2$. Ligand L^1 (20 mg, 29.5 mmol) was treated with zinc(II) triflate (2.1 equivalents) in acetonitrile–chloroform (4:1, 10 cm^3) and stirred for 10 min. The solvent was removed, chloroform was added and the mixture was refluxed for 2 h. The solution was filtered, the residue washed with hot chloroform and water and dried to give $Zn_2L^1{}_2(CF_3SO_3)_4\cdot 5H_2O$ **3** as a light yellow solid (23 mg,78%) (Found: C, 48.5; H, 3.0; N, 7.6. $C_{88}H_{62}F_{12}N_{12}O_{25}S_4Zn_2$ requires C, 48.6; H, 2.9; N, 7.7%). ^{1}H NMR (400 MHz, CD_3CN): δ 2.41 (s, CH_3), 3.98 and 4.77 (AX system, *J* 17.2, $H^{9'}$), 7.90 (d, *J* 7.7, $H^{5''}$), 8.03 (d, *J* 8.0, $H^{5'}$), 8.47 (s, $H^{3,4,9,10}$), 8.49 (dd, *J* 7.7, $H^{4''}$), 8.61 (dd, *J* 8.0, $H^{4'}$), 8.71 (d, *J* 7.7, $H^{3''}$) and 8.88 (d, *J* 8.0 Hz, $H^{3'}$). λ_{max}(log ε) (MeCN) 205 (5.09), 235 (5.11), 272 (4.59), 280 (4.635), 310 (4.68), 322 (4.70), 358 (4.70) and 378 (4.77) nm.

X-Ray crystallography

Diffraction data were collected with a Rigaku AFC7R diffractometer employing graphite-monochromated Cu-Kα radiation (λ 1.541 78 Å) generated from a 12 kW direct-drive rotating anode. Weak reflections with $I < 10.0\sigma(I)$ were rescanned up to 10 times. Stationary background counts were recorded on each side of the reflection, with a ratio of peak counting time to background counting time of 2:1. The intensities of three representative reflections measured every 150 did not change significantly during the course of both data collections. An empirical absorption correction based on azimuthal scans of three reflections was applied to the data and the data were corrected for Lorentz-polarisation effects. Data processing was undertaken with the TEXSAN 1 crystallographic software package.[17] The structures were solved by direct methods[18] and expanded using Fourier techniques with the XTAL software suite.[19]

Crystal data for complex 1. $[(H_2O)ZnL^1{}_2Zn(H_2O)\cdot C_8H_{10}O_2]\cdot xCF_3SO_3\cdot yC_8H_{10}O_2\cdot zH_2O\cdot 4C_2H_3N$, red acicular crystals, 0.30 × 0.03 × 0.03 mm, orthorhombic, space group *Cccm* (no. 66), $Z = 4$, $a = 17.763(3)$, $b = 24.995(8)$, $c = 27.103(2)$ Å, $U = 12\,033(3)$ Å^3, μ(Cu-Kα) = 12.50 cm^{-1}, minimum, maximum transmittance = 0.86, 0.99, *hkl* 0–19, 0–27, 0–29, 2θ 4–115.4, N(unique) = 3659, $N_o[I > 3.00\sigma(I)] = 1222$, $N_{var} = 303$, $R = 0.139$, $R' = 0.132$, maximum residual 0.87 e Å^{-3}.

Data were collected at −100 ± 1 °C with the crystal attached to a glass fibre. The values of *x*, *y* and *z* could not be crystallographically determined and the structure was crystallographically modelled as $C_{111}F_3N_{16}O_{19}SZn_2$.

The crystals containing complex **1** were generally of poor quality and decomposed instantaneously upon removal from the mother-liquor. More remarkably, they also decomposed when co-inserted into a glass capillary with a drop of the mother-liquor and then placed immediately above that drop. Accordingly a data collection was undertaken at −100 ± 1 °C. In a cold room, a red acicular crystal was quickly coated in grease, attached to a glass fibre, transferred to the diffractometer and quenched in a nitrogen cold stream from a Molecular Structure Corporation flexible-tube low-

temperature system. Grease was used to coat the crystal after several unsuccessful attempts using the oil-drop mounting method.[20]

Centred orthorhombic cell constants were obtained from a least-squares refinement against the setting angles of 24 reflections in the range $41.72 < 2\theta < 86.03°$. Omega scans of several intense reflections made prior to data collection had an average width at half-height of 0.27°. The data were collected using ω–2θ scans to a maximum 2θ value of 115.4°. Scans of $(1.26 + 0.35 \tan \theta)°$ were made at a speed of 32.0° min^{-1} (in ω).

Only one of the expected four triflate counter ions was located. Others[11,12] have likewise encountered difficulty in locating all of the expected counter ions for structures of this type, and the difficulty is believed to be due to severe disorder associated with very high solvent mobility in the lattice. The Zn to Zn principal axis of the complex resides on the (i) two-fold axis of space group *Cccm* and the complex is also centrally pierced by the (h) two-fold axis orthogonal to the pyrene ligand bridge. The asymmetric unit thus contains a quarter of the complex. There are a total of two *p*-dimethoxybenzene substrate molecules associated with each complex. There are also four acetonitrile and two water molecules. The refinement model includes two carbon sites assumed to be associated with a disordered and unresolved *p*-dimethoxybenzene substrate molecule residing between complexes. Attempts to add hydrogen atoms at calculated sites led to destabilisation of the refinement and hence hydrogen atoms were not included in the full-matrix least-squares refinement.

One of the two resolved *p*-dimethoxybenzene substrate molecules is intramolecularly π-bound to the pyrene linking units of the complex. The second substrate molecule is intermolecularly π-bound and sandwiched between two complexes. This molecule is disordered over two symmetry-related sites and the intramolecularly bound substrate has two orientations. There are alternating layers of complex and substrate and counter ion stacked in the *c* direction, with the layer containing the counter ion and substrate residing on the (1) mirror plane of space group *Cccm*. That is, the interleaved substrate and the sulfur, carbon, F(1) and O(7) of the anion are located on the (1) mirror plane. The substrate–anion layer is disordered, with alternate substrate and counter ion sites being occupied.

The stacking of the complexes provides large channels running in the *c* direction with approximate volumes of 1600 $Å^3$, and there are two such channels for each unit cell. The twelve triflate ions that have not been located in the unit cell, each with an approximate effective volume of 160 $Å^3$, are assumed to be grossly disordered within these channels.

Crystal data for complex 2. $[(H_2O)ZnL^1{}_2Zn(H_2O)\cdot C_8H_{10}O_2]\cdot x CF_3SO_3\cdot y C_8H_{10}O_2\cdot z H_2O$, orange prism, 0.30 × 0.25 × 0.20 mm, triclinic, space group $P\bar{1}$ (no. 2), $Z = 2$, $a = 16.127(4)$, $b = 26.358(6)$, $c = 13.627(4)$ Å, $\alpha = 99.23(2)$, $\beta = 96.72(2)$, $\gamma = 86.36(2)°$, $U = 5672(2)$ $Å^3$, μ(Cu-Kα) = 18.56 cm^{-1}, minimum, maximum transmittance = 0.58, 0.99, *hkl* 0–17, −27 to 27, −14 to 14, 2θ 4–110.4, $N = 16\,547$, N(unique) = 14 084, $R_{int} = 0.109$, $N_o[I > 3.00\sigma(I)] = 4622$, $N_{var} = 629$, $R = 0.208$, $R' = 0.197$, maximum residual 1.60 e $Å^{-3}$.

The values of *x*, *y* and *z* could not be crystallographically determined, and the structure was crystallographically modelled as $C_{107}F_9N_{12}O_{29.375}S_3Zn_2$.

A crystal of complex **2** was co-inserted with a drop of the mother-liquor into a thin-walled glass capillary. The capillary was sealed and then mounted on the diffractometer. The primitive triclinic cell was obtained from a least-squares refinement against the setting angles of 21 reflections in the range $18.65 < 2\theta < 24.59°$. Omega scans of several intense reflections made prior to data collection had an average width at half-height of 0.43°. Diffraction data were collected at 21 ± 1 °C using ω–2θ scans to a maximum 2θ value of 110.0°, at a speed of 16.0° min^{-1} (in ω).

Only three of the four triflate counter ions expected were unambiguously located. The three fully located triflate ions were refined as rigid bodies, as were the *o*-dimethoxybenzene molecules. Close proximity to a symmetry-related molecule required sites occupancies of 0.5 for the C(101)–C(107) *o*-dimethoxybenzene. The C(11)–C(12)–C(13) and C(29)–C(30)–C(31) angles were restrained to 180°. Twelve sites have been modelled as the oxygen atoms of water molecules; with partial occupancies the total of such oxygens in the asymmetric unit is 5.375. Attempts to add hydrogen atoms at calculated sites led to destabilisation of the refinement and hence hydrogen atoms were not included in the full-matrix least-squares refinement. Sites for atoms heavier than carbon were refined anisotropically, with full-matrix least squares. The C(3), C(41) and C(42) sites were initially refined and then fixed.

Atomic co-ordinates, thermal parameters, and bond lengths and angles have been deposited at the Cambridge Crystallographic Data Centre (CCDC). See Instructions for Authors, *J. Chem. Soc., Dalton Trans.*, 1997, Issue 1. Any request to the CCDC for this material should quote the full literature citation and the reference number 186/557.

Acknowledgements

Financial support from the Australian Research Council (to M. M. H.) is gratefully acknowledged.

References

1 M. Fujita, J. Yazaki and K. Ogura, *J. Am. Chem. Soc.*, 1990, **112**, 5645; *Chem. Lett.*, 1991, 1031; *Tetrahedron Lett.*, 1991, 5589; M. Fujita, S. Nagao and K. Ogura, *J. Am. Chem. Soc.*, 1995, **112**, 1649.
2 P. J. Stang and D. H. Cao, *J. Am. Chem. Soc.*, 1994, **116**, 4981; P. J. Stang, D. H. Cao, S. Saito and A. M. Arif, *J. Am. Chem. Soc.*, 1995, **117**, 6273; P. J. Stang and B. Olenyuk, *Angew. Chem., Int. Ed. Engl.*, 1996, **35**, 732.
3 For recent examples, see A. W. Schwabacher, J. Lee and H. Lei, *J. Am. Chem. Soc.*, 1992, **114**, 7597; J. Linho and A. W. Schwabacher, *J. Am. Chem. Soc.*, 1994, **116**, 8382; A. W. Maverick, M. L. Ivie, J. H. Waggenspack and F. R. Fonczek, *Inorg. Chem.*, 1990, **29**, 2403; M. Albrecht and S. Kotila, *Angew. Chem., Int. Ed. Engl.*, 1995, **34**, 2134; 1996, **35**, 1038; *Chem. Commun.*, 1996, 2309; F. M. Romero, R. Ziessel, A. Dupont-Gervais and A. Van Dorsselaer, *Chem. Commun.*, 1996, 551; M. Fujita, S. Nagao and K. Ogura, *J. Am. Chem. Soc.*, 1995, **117**, 1649.
4 A. Bilyk and M. M. Harding, *J. Chem. Soc., Dalton Trans.*, 1994, 77; A. Bilyk, M. M. Harding, P. Turner and T. W. Hambley, *J. Chem. Soc., Dalton Trans.*, 1994, 2783; A. Bilyk, M. M. Harding, P. Turner and T. W. Hambley, *J. Chem. Soc., Dalton Trans.*, 1995, 3905.
5 A. Bilyk and M. M. Harding, *J. Chem. Soc., Chem. Commun.*, 1995, 1697.
6 P. Jutzi and U. Gilige, *J. Organomet. Chem.*, 1983, **246**, 163.
7 J. Uenishi, K. Tanaka, S. Wakabayashi and S. Oae, *Tetrahedron Lett.*, 1990, **31**, 4625; J. Uenishi, K. Tanaka, S. Nishiwaki, S. Wakabayashi, S. Oae and H. Tsukube, *J. Org. Chem.*, 1993, **58**, 4382.
8 G. Garcia and J. Vilarrasa, *Tetrahedron Lett.*, 1986, **27**, 639.
9 W. S. V. Kwan, L. Atanasoska and L. L. Miller, *Langmuir*, 1991, **7**, 1419; T. M. Dietz, S. Takenaka, M. Manabe, M. Yokoyama, M. Nishi, J. Tanaka and H. Kondo, *Chem. Commun.*, 1996, 379; J. Jazwinski, J. A. Blacker, J.-M. Lehn, M. Cessario, J. Guilhem and C. Pascard, *Tetrahedron Lett.*, 1987, **28**, 6057; A. Osuka, H. Shiratori, R. Yoneshima, T. Okada, S. Taniguchi and N. Matage, *Chem. Lett.*, 1995, 913.
10 E. C. Taylor, J. E. Macor and J. L. Pont, *Tetrahedron*, 1987, **43**, 5145.
11 C. J. Zhong, W. S. V. Kwan and L. L. Miller, *Chem. Mater.*, 1992, **4**, 1423.
12 M. Fujita, O. Sasaki, T. Mitsuhashi, J. Yazaki, K. Yamaguchi and K. Ogura, *Chem. Commun.*, 1996, 1535.
13 B. Olenyuk, J. A. Whiteford and P. J. Stang, *J. Am.Chem. Soc.*, 1996, **118**, 8221.
14 C. K. Johnson, ORTEP, Report ORNL-5138, Oak Ridge National Laboratory, Oak Ridge, TN, 1976.

15 C. A. Hunter, *Angew. Chem., Int. Ed. Engl.*, 1993, **32**, 1584; P. C. Kearney, L. S. Mizoue, R. A. Kumpf, J. E. Forman, A. McCurdy and D. A. Dougherty, *J. Am. Chem. Soc.*, 1993, **115**, 9907; A. Galan, D. Andrew, A. E. Echavarren, P. Prados and J. de Mendoza, *J. Am. Chem. Soc.*, 1992, **114**, 1511; B. J. Whitlock and H. W. Whitlock, *J. Am. Chem. Soc.*, 1990, **112**, 3910; J. Jazwinski, A. J. Blacker, J.-M. Lehn, M. Cesario, J. Guilhem and J. Pascard, *Tetrahedron Lett.*, 1987, 6057.
16 G. R. Newkome, H. W. Lee and F. R. Fronzek, *Isr. J. Chem.*, 1986, **27**, 87.
17 TEXSAN, Crystal Structure Analysis Package, Molecular Structure Corporation, Houston, TX, 1985 and 1992.
18 G. M Sheldrick, SHELXS 86, in *Crystallographic Computing 3*, eds. G. M. Sheldrick, C. Kruger and R. Goddard, Oxford University Press, 1985, p. 175.
18 XTAL 3.4, *Reference Manual*, eds. S. R. Hall and J. M. Stewart, Universities of Western Australia and Maryland, 1995.
20 H. Hope, *Acta Crystallogr., Sect. B*, 1988, **44**, 22.

Received 7*th April* 1997*; Paper* 7/02378B

© Copyright 1997 by the Royal Society of Chemistry